Mesoporous Basic Catalysts

Highly Ordered Mesoporous Silicon Oxynitride Materials as Base Catalysts**

*Yongde Xia and Robert Mokaya**

The discovery of mesoporous silicates by researchers at the Mobil company a decade ago, was a significant step in expanding the range of ordered zeolite-type materials beyond the microporous range and into the mesoporous regime.[1] However, purely siliceous mesoporous materials have neutral silica frameworks, which limits their applications in the fields of catalysis, ion exchange or adsorption. To obtain mesoporous solids with potential for use as catalysts, it is necessary to introduce heteroatoms and/or organic functional moieties that have specific active sites, into or onto the silica framework.[2] For example when Si in a mesoporous silica framework is substituted by other metal ions, M^{n+}, (where M^{n+} may be tetravalent, Ti^{4+}, V^{4+}, Sn^{4+} or trivalent, Al^{3+}, Fe^{3+}, Ga^{3+})[3,4] the framework either maintains electroneutrality (for M^{4+}) or acquires an overall negative charge (for M^{3+}) that may be compensated for by cations (e.g. protons). The M^{4+} ion substituted silica materials may be used as redox catalysts while M^{3+} ion substituted materials can function as solid acid or basic catalysts when protons or alkali/alkaline earth cations are the charge balancing ions respectively. In both cases the number and strength of the active sites generated generally depends on the amount and nature of the heteroatom. An extensively studied example is that of aluminum-containing mesoporous silica materials, which have attracted attention because of their potential application as solid acid catalysts.[4]

Although most metal-ion (i.e., cation) substituted mesoporous silica frameworks can be prepared by direct synthesis or by post-synthesis grafting methods, it is now thought that grafted materials are more catalytic active than their directly prepared analogues because of the higher accessibility of active sites.[5] However, in contrast to the abundance of research on cation-modified mesoporous silica materials, there are very few reports on framework "anion-modified" materials. Anion modified frameworks have been extensively studied for other classes of materials. For example when amorphous silica,[6] microporous aluminosilicate/aluminophosphate,[7] or aluminum vanadate[8] are treated with ammonia at high temperatures, the oxygen in their framework is partially displaced by nitrogen or NH_x species (to generate oxynitride frameworks), which have active sites capable of catalysing base-catalyzed reactions. As a consequence of the

[*] Dr. R. Mokaya, Dr. Y. Xia
School of Chemistry
University of Nottingham
University Park, Nottingham NG7 2RD (UK)
Fax: (+44) 115-951-3562
E-mail: r.mokaya@nottingham.ac.uk

[**] The authors are grateful to the EPSRC for financial support and the Royal Society for an equipment grant. The assistance of Dr P. Licence with the catalysis work is gratefully acknowledged.

 DOI: 10.1002/ange.200350978

amorphous nature of the pore walls of mesoporous silica materials, NH_x species can be immobilized/incorporated onto the surface of mesoporous silica frameworks via high-temperature treatment in the presence of ammonia or nitrogen.[6,9] This affords new types of mesostructured solid base materials with high surface area and pore volume.

Basic mesoporous materials may be prepared by one of three other routes;[10] 1) cation exchange with alkali (e.g., Na^+, K^+, Cs^+) metal ions, 2) impregnation with basic salts and 3) functionalisation with organic moieties (e.g., amines), which are basic. These methods, however, suffer from various disadvantages, such as competition from acidic sites and a low cation exchange capacity (which limits number of possible basic sites) for route 1), while route 2) and 3) suffer from problems with leaching along with structural degradation and a drastic decrease in textural properties (surface area, pore volume and pore size).[2,10] Herein, we report a synthesis route to mesoporous base catalysts, which exhibit excellent mesostructural ordering and considerable catalytic activity. We present the synthesis of structurally well-ordered anion (NH_x species) modified mesoporous-silica materials and also report on their catalytic activity for the base catalysed Knoevenagel condensation reaction. The materials were obtained by reacting cubic phase mesoporous silica with ammonia (a process hereinafter referred to as nitridation) at high temperature to obtain nitrogen-containing mesoporous-silica materials. The high structural ordering of the nitrogen-containing mesoporous materials reported here benefits from the use of high-quality sodium-free Si-MCM-48 as the starting material.[11] The use of Na-free Si-MCM-48 allowed us to use an optimised (i.e., relatively high) nitridation temperature—the presence of sodium ions in mesoporous silicas is known to have a detrimental effect on thermal/hydrothermal stability.[11,12] An optimised nitridation temperature preserved the mesoporous structure from collapse and allowed the ammonia molecules to react efficiently with silanol groups and/or bridging oxygen on the host Si-MCM-48 material. We show that NH_x species are incorporated onto the N-containing MCM-48 materials and generate basic sites, which exhibit considerable catalytic activity for the Knoevenagel condensation reaction. The resulting well-ordered mesoporous oxynitride materials, which have high surface area and pore volume, are likely to be attractive as alternative basic catalysts especially for large molecule transformations.

The structural ordering of the parent Si-MCM-48 and ammonia treated MCM-48 materials was assessed by powder X-ray diffraction (XRD). As shown in Figure 1, all the XRD patterns are typical for highly ordered MCM-48 materials with an intense *d* spacing (211) diffraction peak and several well-resolved higher order peaks in the 2θ range of 3–6°, which can be indexed to *Ia3d* cubic structure.[1] The synthesized and calcined Si-MCM-48 materials have different d_{211} spacing (37.6 Å and 35.4 Å respectively), which indicates a 6% contraction of the MCM-48 lattice after calcination. However, after being subjected to thermal treatment at 900 °C in a flow of ammonia gas, the resulting N-containing materials (designated as N-MCM-48A and N-MCM-48B for materials derived from nitridation of calcined or as-synthesized Si-MCM-48 respectively) exhibit similar d_{211} spacing of about

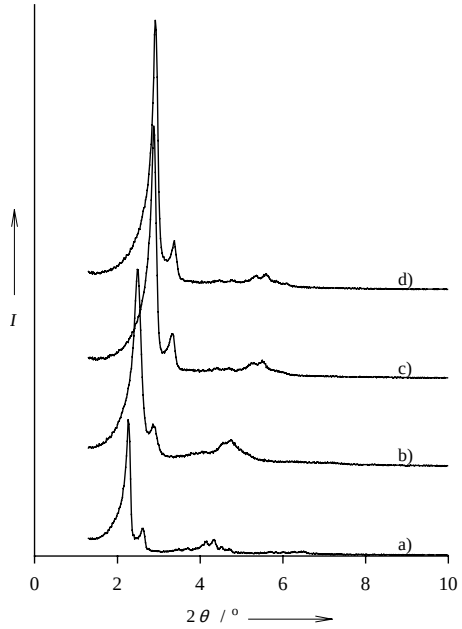

Figure 1. Powder XRD patterns of a) as-synthesized Si-MCM-48, b) calcined Si-MCM-48 and nitrided c) N-MCM-48A and d) N-MCM-48B materials.

30.3 Å. Noteworthy, when the parent Si-MCM-48 was subjected to heat treatment at 900 °C in air for the same duration as for the nitridation reaction (i.e., 20 h) it was virtually destroyed (surface area and pore volume reduced to 62 $m^2 g^{-1}$ and 0.07 $cm^3 g^{-1}$ respectively). This implies that an ammonia atmosphere is an important factor in maintaining structural ordering during nitridation. Interestingly, the intensity of the d_{211} diffraction peak for both nitrided materials is higher than that of the respective parent materials as shown in Figure 1.

The nitridation reaction occurs according to the following schemes

$$\equiv Si{-}OH + NH_3 \rightarrow \equiv Si{-}NH_2 + H_2O$$

and/or

$$\equiv Si{-}O{-}Si\equiv + NH_3 \rightarrow \equiv Si{-}NH{-}Si\equiv + H_2O \text{ or}$$
$$\equiv Si{-}NH_2 + \equiv Si{-}OH$$

Given that synthesized mesoporous silica materials have a higher concentration of silanol groups than their calcined analogues,[13] it is reasonable to expect sample N-MCM-48B, which was obtained by nitridation of the synthesized Si-MCM-48, to have a higher NH_x density on its surface. Elemental analysis (see Table 1) confirmed that sample N-MCM-48B contained 14.7 wt % of N, which corresponded to a Si:N:O molar ratio of 1:0.65:1.025 while N-MCM-48A obtained by nitridation of calcined Si-MCM-48 had a N content of 11.4 wt % which is close to a Si:N:O molar ratio of 1:0.5:1.25.

The quality and structural ordering of the parent Si-MCM-48 and N-MCM-48 materials were also evaluated by N_2 sorption studies. The N_2 sorption isotherms of the materials

Table 1: Elemental composition, *d* spacing and textural properties of studied MCM-48 materials.

Sample	N content [wt%]	d_{211} spacing [Å]	Surface area per gram [$m^2 g^{-1}$]	Pore volume per gram [$cm^3 g^{-1}$]	Pore size [Å]
Si-MCM-48		35.4	1247	1.10	34.1
N-MCM-48A	11.4	30.4	1340	0.65	20.0
N-MCM-48B	14.7	30.3	1487	0.66	17.8

are presented in Figure 2 and the corresponding textural properties are summarized in Table 1. Both Si-MCM-48 and N-MCM-48 exhibit type IV isotherms with a typical capillary condensation step into uniform pores without hysteresis. This indicates that both Si-MCM-48 and the N-MCM-48 samples

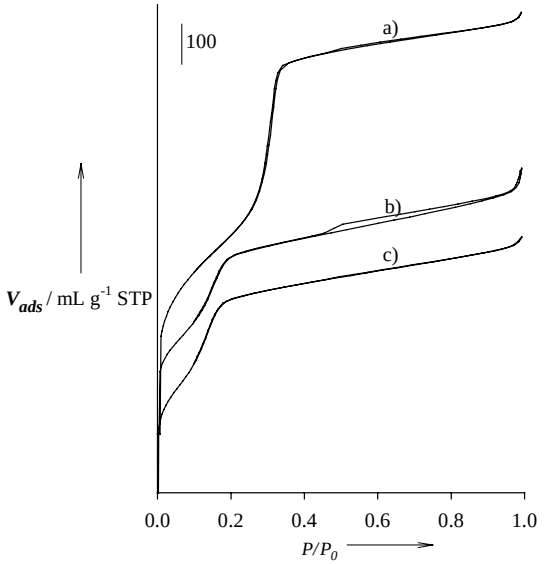

Figure 2. Nitrogen sorption isotherms of a) calcined Si-MCM-48 and nitride, b) N-MCM-48A, and c) N-MCM-48B materials. P/P_0 is partial pressure.

have good structural ordering. The capillary condensation step for Si-MCM-48 is in the relative pressure range 0.25–0.35 while the N-MCM-48 samples exhibit pore filling steps in the relative pressure range 0.15–0.22, thus indicating that the high-temperature treatment in ammonia results in a significant reduction in pore size. As shown in Table 1 the pore size of the N-MCM-48 materials is in the super-microporous to lower mesopore range. The reduction in pore size after nitridation arises from contraction of the lattice occasioned by the relatively severe thermal treatment at 900 °C. Indeed as noted above, extended (20 h) calcination at 900 °C virtually destroys the parent Si-MCM-48 material. Pore-wall thickening after nitridation also contributes to pore size reduction. The wall thickness of Si-MCM-48 was 11 Å compared to 14.1 Å and 15.1 Å for N-MCM-48A and N-MCM-48B respectively. However, the structural changes resulting from the thermal treatment in ammonia are not necessarily at the expense of pore uniformity or structural ordering as evidenced in Figure 1 and Figure 2.

Both Si-MCM-48 and the N-MCM-48 materials have a surface area per gram in the range 1200–1500 $m^2 g^{-1}$, which is typical for highly ordered MCM-48 materials.[1,11] However, the N-MCM-48 materials retain only 60% of the pore volume of the parent Si-MCM-48 material. This is consistent with the pore size contraction observed. The pore size contraction is expected to have a much greater effect on the pore volume than on the surface area, which is observed to increase slightly after nitridation. We note that a slight increase in surface area after nitridation has previously been observed for other types of porous materials.[6–8] The overall picture that emerges from the textural parameters is that upon nitridation of well-ordered Si-MCM-48, the resulting N-MCM-48 materials retain good structural ordering despite a significant decrease in pore volume and pore size.

The excellent structural ordering of the N-MCM-48 materials was also evidenced by transmission electron microscopy (TEM) as shown by the representative TEM image in Figure 3. Well-ordered pore channels are observed, thus indicating the excellent ordering of the nitrided materials. From the TEM micrograph it is possible to estimate a pore

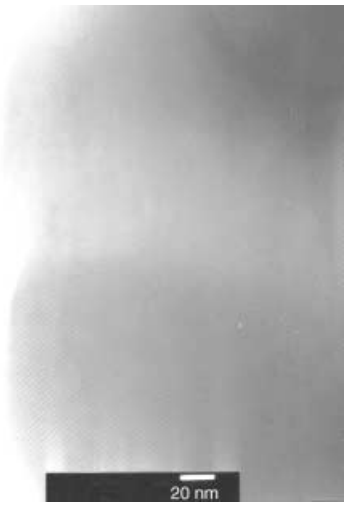

Figure 3. Representative TEM image of nitrided N-MCM-48A.

channel diameter of 2 nm, which is similar to the pore size obtained from nitrogen sorption studies (Table 1). The particle morphology of the Si-MCM-48 and N-MCM-48 materials was investigated by scanning electron microscopy (SEM) and representative SEM images are shown in Figure 4. The Si-MCM-48 material exhibits well-formed cubic (rhombic dodecahedral) crystal-like particles (Figure 4a) of diameter in the range of 0.5–2 μm. The N-MCM-48A material (Figure 4b) also displays cubic crystal-like particles of diameter in the range 0.5–1 μm while the N-MCM-48B sample is made up of cubic particles, which, in some cases, appear to be bunched together but with a discernable particle size of 0.5–2 μm as shown in Figure 4c. It is worthwhile to note that the

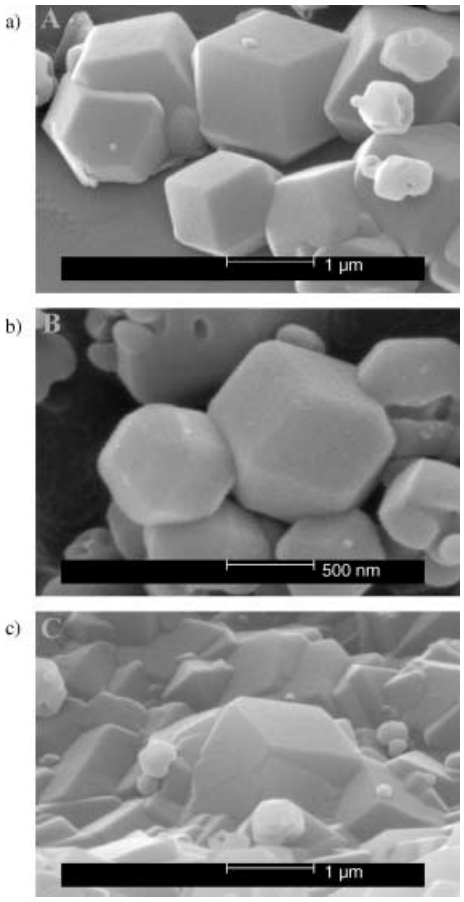

Figure 4. Representative SEM images of a) calcined Si-MCM-48 and nitrided b) N-MCM-48A and c) N-MCM-48B materials.

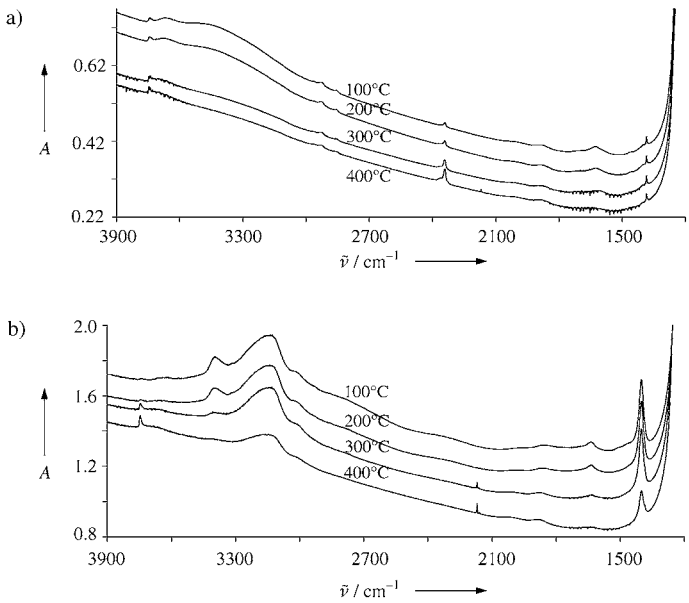

Figure 5. IR spectrum of a) calcined Si-MCM-48 and b) nitrided N-MCM-48A samples evacuated in vacuo at the temperatures shown. A = Absorbance.

"bunching" appearance shown in Figure 4c for sample N-MCM-48B is also observed for the N-MCM-48A and Si-MCM-48[11] and is therefore not a unique feature of sample N-MCM-48B. The particle morphology is therefore largely maintained after nitridation. The retention of particle morphology after nitridation has previously been reported for other types of porous oxides.[14]

Infrared spectroscopy was used to ascertain the presence of NH or NH_2 groups on the surface of the nitrided MCM-48 materials. Pure silica MCM-48 (Figure 5a) exhibits very low absorbance bands from Si–OH ν(OH) at 3743 cm^{-1} and adsorbed water at 3673 cm^{-1} and 1620 cm^{-1} along with several small peaks attributed to ν(CH) and δ(CH) which were also observed at about 2900 cm^{-1} and 1384 cm^{-1} arising from the presence of trace amount of surfactant on the sample. The peaks at 2340 cm^{-1} and 1860 cm^{-1} come from the overtones and combination bands of lattice vibrations. The main effect of increasing the evacuation temperature from 100 °C to 400 °C was the gradual decrease of the intensity of peaks attributed to adsorbed water. The N-containing MCM-48 sample (N-MCM-48A, Figure 5b) on the other hand displays several very strong absorbance bands at 3396 cm^{-1} and 3147 cm^{-1}, which are attributed to the stretching NH bands ν(N–H).[6,7,15] The strong absorbance bands at 1401 cm^{-1} and 1639 cm^{-1} can be assigned to $\delta_{as}(NH_4^+)$ of NH_3 bonded to a Si–OH hydroxyl group and the presence of adsorbed NH_3 or/and water.[8,15] On increasing the evacuation temperature from 100 °C to 400 °C, the intensities of absorbance bands from all the NH_x species (including ν(NH) from Si–NH–Si and Si–NH_2 at 3396 cm^{-1} and 3147 cm^{-1} and $\delta_{as}(NH_4^+)$ from NH_4^+ at 1401 cm^{-1}) decrease gradually. The bands at 3147 cm^{-1} and 1401 cm^{-1} are, however, still observed after thermal treatment at 400 °C in a vacuum, thus indicating that at least part of the NH_x species incorporated into the mesoporous silica are thermal stable up to 400 °C.

The Knoevenagel condensation reaction has been shown to be a useful probe of the basicity of solids when carried out with a series of methylene groups of varying pK_a, and it has been used to evaluate the basicity of solid bases such as amorphous silicon oxynitride, silicon imidonitride or aluminophosphates oxynitride.[6–8,16,17] To explore the catalytic properties of the MCM-48 silicon oxynitride materials, Knoevenagel condensation between benzaldehyde and malononitrile (Scheme 1) was preformed at 60 °C under an inert

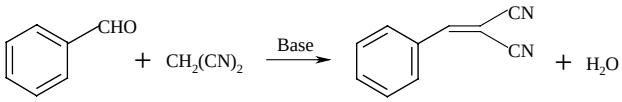

Scheme 1. Knoevenagel condensation reaction between benzaldehyde and malononitrile.

atmosphere. The catalytic data is presented in Figure 6. It was found that whilst pure silica MCM-48 exhibited negligible catalytic activity, N-MCM-48 materials were active catalysts for the test reaction. After a 3 h reaction time, both N-MCM-48A and N-MCM-48B achieved conversions of 78% and 96% respectively to give 1,1-dicyanophenylethylene with a selectivity of 100%. The higher conversion over N-MCM-48B is consistent with its higher nitrogen content. No Michael

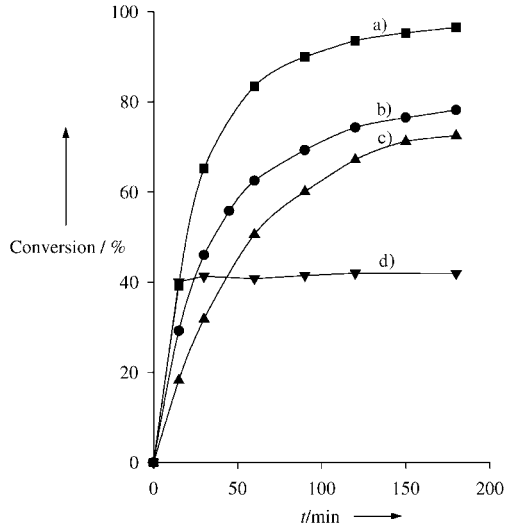

Figure 6. Conversion as a function of time in the Knoevenagel condensation reaction of malononitrile with benzaldehyde at 60 °C in toluene solution catalyzed by; a) N-MCM-48B, b) N-MCM-48A, c) MgO and conversion as a function of time d) after removal of the catalyst (N-MCM-48B) by filtration of the reaction mixture. The reaction had previously been allowed to proceed for 15 min in the presence of the N-MCM-48B catalysts during which a conversion of 40% was attained. t = Reaction time.

addition products, which involve the reaction of malononitrile with the double bond of the 1,1-dicyanophenylethylene, were detected under our reaction conditions. The Michael addition reaction is known to require stronger basic sites or higher reaction temperatures than Knoevenagel condensation,[17] thus suggesting that either there are no strong basic sites on the surface of N-MCM-48 materials, or that higher temperatures are required for Michael addition to occur.[17] The latter is more likely since we did not observe Michael addition even for a commercially available MgO catalyst which is known to have strong basic sites. The absence of Michael addition at a reaction temperature of 60 °C is consistent with previous results.[17] Noteworthy, the catalytic activities achieved by the N-MCM-48 materials were higher than that of the commercially available MgO catalyst (see Figure 6). We infer that the higher overall conversion on the N-MCM-48 catalysts arises from a higher content of basic site (compared to MgO). This inference is consistent with the higher surface area and pore volume per gram of the mesostructured N-MCM-48 oxynitride materials (1200–1500 $m^2 g^{-1}$ and ca. 0.65 $cm^3 g^{-1}$) compared to 44 $m^2 g^{-1}$ and 0.26 $cm^3 g^{-1}$ for the commercial MgO catalyst.

It is important to note that water is one of the products of the Knoevenagel condensation reaction and that the N-MCM-48 oxynitrides would, to some extent, be hydrolytically sensitive to water. Any hydrolysis of the oxynitrides would yield ammonia. Furthermore, since the N-MCM-48 materials were nitrided under a flow of ammonia and given that ammonia is known to catalyze the Knoevenagel condensation reaction homogeneously, it was important to verify that the observed catalytic activity was from the solid N-MCM-48 oxynitride materials and not ammonia. Therefore a control experiment was performed as follows; a catalytic reaction was carried out with N-MCM-48B as catalyst and stopped after 15 min at 40% conversion. The reaction mixture was then cooled and filtered to remove the solid N-MCM-48B catalyst after which the catalyst free filtrate was heated to 60 °C and conversion monitored as a function of time. As shown in Figure 5d, no increase in conversion was observed (i.e., the composition of the filtrate remained unchanged). This observation from the control experiment rules out any contribution to the observed catalytic activity from a homogeneously catalyzed reaction of ammonia. We therefore believe[8,16] that the presence of NH_x species on the N-MCM-48 materials is responsible for the observed catalytic activity.

In summary, we have presented here an attractive route for the preparation of mesoporous base catalysts that are well ordered and have a high surface area, pore volume and catalytic activity. The resulting materials are both truly mesoporous and, as far as we can tell, entirely basic in character. They exhibit considerable thermal stability and do not appear to suffer from leaching (of the basic sites) during catalysis. The method described herein is not limited to MCM-48 and may be used to prepare mesoporous oxynitride materials from other types of mesostructured silicas or metal substituted silicas. There is also scope, by the nitridation route, to prepare acid/base mesoporous materials where the ratio of acidity to basicity is readily controlled. Such highly ordered novel mesoporous oxynitride or acid/base materials with high surface area and pore volume are attractive and may find use as alternative solid catalytic materials.

Experimental Section

High-quality sodium-free Si-MCM-48 was synthesized by using a method in which cetyltrimethylammonium hydroxide (CTAOH) was used simultaneously as a structure director and also to control the pH of the synthesis gel.[11] Typically, 2.14 g of fumed silica was added to 30 g of a 10% CTAOH stirring solution. The mole ratio of the gel mixture of SiO_2:CTAOH:H_2O was 1:0.28:42. After the reaction mixture was stirred for 2 h at room temperature, it was transferred to a teflon-lined autoclave and heated at 135 °C for 24 h. The autoclave was cooled to room temperature and the solid product isolated by filtration and repeatedly washed with a large amount of distilled water. After the product was air-dried at room temperature, part of the dry material was calcined in air at 550 °C for 6 h to yield calcined Si-MCM-48. For nitridation, 0.2 g of calcined or synthesized Si-MCM-48 was placed in an alumina boat and inserted into a flow-through tube furnace. Prior to thermal treatment, the tube furnace was purged by Ar for 30 min, then further purged with NH_3 for another 30 min. The NH_3 flow rate was 100 mL min^{-1}, the temperature of the furnace was increased at a ramp rate of 5 K min^{-1} to 900 °C and maintained for 20 h under the NH_3 atmosphere. The furnace was then cooled down to RT and purged again with Ar for 30 min. The nitrided sample obtained from calcined Si-MCM-48 was designated N-MCM-48A and that obtained from synthesized Si-MCM-48 was designated N-MCM-48B.

Powder XRD analysis was performed by using a Philips 1710 powder diffractometer with Cu K_α radiation (40 kV, 40 mA). Nitrogen sorption isotherms and textural properties of the materials were determined at 77 K by using nitrogen in a conventional volumetric technique by a Coulter SA3100 sorptometer. Before analysis the samples were oven dried at 150 °C and evacuated for 12 h at 200 °C

under vacuum. The surface area was calculated using the BET method based on adsorption data in the partial pressure (P/P_0) range 0.05–0.2 and total pore volume was determined from the amount of the nitrogen adsorbed at $P/P_0 \approx 0.99$. Elemental analysis was carried out on the nitrided samples by using a CHNS analyzer (Fishons EA 1108). Infrared spectra were recorded using a Perkin Elmer 2000 FTIR spectrometer on self-supporting sample wafers in a pyrex vacuum IR cell. Prior to the collection of spectra the samples were heated in the cell for 2 h at increasing temperature, after which the spectra were recorded at room temperature. Scanning electron microscopy (SEM) images were recorded using a JEOL JSM-820 scanning electron microscope. Samples were mounted using a conductive carbon double-sided sticky tape. A thin (ca. 10 nm) coating of gold sputter was deposited onto the samples to reduce the effects of charging. Transmission electron microscopy (TEM) images were recorded on a JEOL 2000-FX electron microscope operating at 200 kV. Samples for analysis were prepared by spreading them on a holey carbon film supported on a grid.

The Knoevenagel condensation test reactions were performed under an inert atmosphere (N_2), in a flask that was fitted with a reflux condenser. The flask containing a mixture of redistilled benzaldehyde (10 mmol), malononitrile (10 mmol) and 40 mL toluene was immersed in an oil bath and the reaction mixture was stirred with a bar magnet. Once the mixture reached the reaction temperature (60 °C), 0.05 g catalyst was added into the flask. Samples of the reaction mixture were then periodically withdrawn by a filtering syringe and analyzed by a GC-17A gas chromatography to obtain the extent of conversion (%) as a function of reaction time.

Received: January 21, 2003 [Z50978]

Keywords: basicity · heterogeneous catalysis · knoevenagel condensation · mesoporous materials · silicon

[1] a) C. T. Kresge, M. E. Leonowicz, W. J. Roth, J. C. Vartuli, J. S. Beck, *Nature* **1992**, *359*, 710; b) J. S. Beck, J. C. Vartulli, W. J. Roth, M. E. Leonowicz, C. T. Kresge, K. D. Schmitt, C. T. W. Chu, D. H. Olson, E. W. Sheppard, S. B. McCullen, J. B. Higgings, J. L. Schlenker, *J. Am. Chem. Soc.* **1992**, *114*, 10834.

[2] a) A. P. Wight, M. E. Davis, *Chem. Rev.* **2002**, *102*, 3589; b) J. Y. Ying, C. P. Mehnert, M. S. Wong, *Angew. Chem.* **1999**, *111*, 58; *Angew. Chem. Int. Ed.* **1999**, *38*, 56; c) A. Corma, *Chem. Rev.* **1997**, *97*, 2373; d) D. T. On, D. Desplantier-Giscard, C. Danumah, S. Kaliaguine, *Appl. Catal. A* **2001**, *222*, 299.

[3] a) P. T. Tanev, M. Chibwe, T. J. Pinnavaia, *Nature* **1994**, *368*, 321; b) P. T. Tanev, T. J. Pinnavaia, *Science* **1995**, *267*, 865; c) J. V. Walker, M. Morey, H. Carlsson, A, Davidson, G. D. Stucky, *J. Am. Chem. Soc.* **1997**, *119*, 6921; d) L. X. Dai, K. Tabata, E. Suzuki, T. Tatsumi, *Chem. Mater.* **2001**, *13*, 208; e) R. Mokaya, W. Jones, *J. Catal.* **1997**, *172*, 211; f) T. M. Abdel Fattah, T. J. Pinnavaia, *J. Chem. Soc. Chem. Commun.* **1996**, 665; g) B. Echchahed, A. Moen, D. Nicholson, L. Bonneviot, *Chem. Mater.* **1997**, *9*, 1716; h) P. van der Voort, E. F. Vansant, *J. Phys. Chem. B* **1999**, *103*, 10102; i) M. Froba, R. Kohn, G. Bouffaud, *Chem. Mater.* **1999**, *11*, 2858.

[4] a) R. Mokaya, *Angew. Chem.* **1999**, *111*, 3079; *Angew. Chem. Int. Ed.* **1999**, *38*, 2930; b) R. Mokaya, *Adv. Mater.* **2000**, *12*, 1681; c) R. Mokaya, *ChemPhysChem* **2002**, *3*, 360; d) A. S. O'Neil, R. Mokaya, M. Poliakoff, *J. Am. Chem. Soc.* **2002**, *124*, 10636; e) S. C. Shen, S. Kawi, *Langmuir* **2002**, *18*, 4720.

[5] R. D. Oldroyd, J. M. Thomas, T. Maschmeyer, P. A. MacFaul, D. W. Snelgrove, K. U. Ingold, D. M. Wayner, *Angew. Chem.* **1996**, *108*, 2966; *Angew. Chem. Int. Ed. Engl.* **1996**, *35*, 2787.

[6] a) P. W. Lednor, R. Derutter, *J. Chem. Soc. Chem. Commun.* **1991**, 1625; b) P. W. Lednor, *Catal. Today* **1992**, *15*, 243; c) G. Busca, V. Losenzelli, G. Porcile, *Mater. Chem. Phys.* **1986**, *14*, 123.

[7] a) M. J. Climent, A. Corma, V. Fornes, A. Frau, R. Guil-Lopez, S. Iborra, J. Primo, *J. Catal.* **1996**. *163*, 392; b) P. Grange, P. Bastians, R. Conanec, R. Marchand, Y. Laurent, *Appl. Catal. A* **1994**, *114*, L191; c) S. Ernst, M. Hartmann, S. Sauerbeck, T. Bongers, *Appl. Catal. A* **2000**, *200*, 117; d) J. Xiong, Y. Ding, H. Zhu, L. Yan, X. Liu, L. Lin, *J. Phys. Chem. B* **2003**, *107*, 1366.

[8] a) H. M. Wiame, C. M. Cellier, P. Grange, *J. Phys. Chem. B* **2000**, *104*, 591; b) H. Wiame, C. Cellier, P. Grange, *J. Catal.* **2000**, *190*, 406.

[9] a) M. P. Kapoor, S. Inagaki, *Chem. Lett.* **2003**, *32*, 94; b) H. Yoshida, Y. Inaki, Y. Kajita, K. Ito, T. Hattori, *Stud. Surf. Sci. Catal.* **2002**, *143*, 837; c) J. E. Haskouri, S. Cabrera, F. Sapina, J. Latorre, C. Guillen, A. Beltran-Porter, D. Beltran-Porter, M. D. Marcos, P. Amoros, *Adv. Mater.* **2001**, *13*, 192.

[10] J. Weitkamp, M. Hunger, U, Rymsa, *Microporous Mesoporous Mater.* **2001**, *48*, 255.

[11] Y. D. Xia, R. Mokaya, *J. Mater. Chem.* **2003**, *13*, 657.

[12] T. R. Pauly, V. Petkov, Y. Liu, S. J. L. Billinge, T. J. Pinnavaia, *J. Am. Chem. Soc.* **2002**, *124*, 97.

[13] J. Chen, Q. Li, R. Xu, F. Xiao, *Angew. Chem.* **1995**, *107*, 2898; *Angew. Chem. Int. Ed. Engl.* **1995**, *34*, 2694.

[14] a) T. Suehiro, J. Tatami, T. Meguro, S. Matsuo, K. Komeya, *J. Eur. Ceram. Soc.* **2002**, *22*, 521; b) T. Suehiro, J. Tatami, T. Meguro, K. Komeya, S. Matsuo, *J. Am. Ceram. Soc.* **2002**, *85*, 715.

[15] a) S. Delsarte, M. A. Centeno, P. Grange, *J. Non-Cryst. Solids* **2002**, *297*, 189; b) R. L. Puurunen, A. Root, P. Sarv, M. M. Viitanen, H. H. Brongersma, M. Lindblad, A. O. I. Krause, *Chem. Mater.* **2002**, *14*, 720; c) T. Blasco, A. Corma, L. Fernandez, V. Fornes, R. Guil-Lopez, *Phys. Chem. Chem. Phys.* **1999**, *1*, 4493.

[16] J. S. Bradley, O. Vollmer, R. Rovai, U. Specht, F. Lefebvre, *Adv. Mater.* **1998**, *10*, 938.

[17] M. J. Climent, A. Corma, R. Guil-Lopez, S. Iborra, *Catal. Lett.* **2001**, *74*, 161.

